

Supplementary Material

Deciphering the spatiotemporal trade-offs and synergies between ecosystem services and their socio-ecological drivers in the plain river network area

Haishun Xu*, Jiaqing Cheng, Yanping Guo, Tongxin Zhong, Jinguang Zhang

College of Landscape Architecture, Nanjing Forestry University, Nanjing, China, 210037

* **Correspondence:** Haishun Xu: xuhaishun@njfu.edu.cn

1 Ecosystem Services Assessment

(1) Carbon storage (CS)

The relevant parameters of carbon storage were mainly obtained by referring to the relevant literature (Liu et al., 2010; Zhou et al., 2019; Cai and Peng, 2021) with the Jianghuai region where the study area was located and referring to the relevant instructions in the *2019 Revised 2006 IPCC Guidelines for National Greenhouse Gas Inventories*.

Table S.1 Carbon pools for different LULC types in Xinghua (t/hm²).

lucode	LULC_name	C _{above}	C _{below}	C _{soil}	C _{dead}
11	Paddy Field	1.8873	1.2457	8.6759	0.241
12	Dryland	1.8873	1.2457	8.6759	0.241
24	Woodland	3.6339	0.7268	12.0758	0.3354
31	Grassland	1.7374	2.0849	10.5847	0.294
41	Canal	3.25	0	8.11	0
42	Lake	3.25	0	8.11	0
43	Reservoir pit	3.25	0	8.11	0

46	Beach land	3.25	0	0	0
51	Urban land	1.6153	0.3231	7.292	0
52	Rural land	1.6153	0.3231	7.292	0
53	Other construction land	1.6153	0.3231	7.292	0

where

lucode is the LULC codes from the LULC raster, C_{toil} is the total carbon storage (t/hm^2), C_{above} is the aboveground biomass (t/hm^2), C_{below} is the belowground biomass (t/hm^2), C_{soil} is the soil carbon density (t/hm^2), and C_{dead} is the carbon density of dead organic matter (t/hm^2).

(2) Habitat quality (HQ)

The habitat quality module of the InVEST model can analyse external threat factors and their intensity, combining the sensitivity of each land use type to the threat source to evaluate the habitat quality (Hu et al., 2023). The calculation formula was as follows:

$$D_{xj} = \sum_{r=1}^R \sum_{y=1}^{Y_r} (w_r / \sum_{r=1}^R w_r) r_y i_{rxy} \beta_x S_{jr}$$

$$Q_{xj} = H_j \left[1 - \left(\frac{D_{xy}^z}{D_{xy}^z + k^z} \right) \right]$$

where D_{xj} , Q_{xj} , and H_j are overall threat degree, habitat quality, and habitat suitability, respectively. j is the land use type, x is the raster pixel, r is the number of threat sources, y is the raster in the threat source r , w_r is the weight of each threat source, r_y is the coercive value of y , β_x is the level of habitat resistance to disturbance, S_{jr} is the degree of sensitivity to the threat factor for the different land use types. z is the normalised constant, usually 2.5; k is the half-saturation constant, usually half of the maximum habitat degradation, and k is the weight of each threat source.

During the actual use of the HQ module, it was necessary to input the LULC maps, threat rasters, sensitivity of the land cover types to each threat, and threat parameters in the corresponding section of the module. The processing of threat rasters and the associated parameters were provided below.

Threat Rasters: threats that were closely related to human activities, i.e., arable land (paddy and dry land), urban land, and rural land, were selected in this study. (Figure S.1)

Paddy fields were taken as an example. In GIS, first of all, the nodata in LULC map was reclassified and assigned the value of 0, and then the raster was converted to a surface through the conversion tool. The value field was added in the attribute table of vector data, then the rows where "paddy field" was located were filtered out according to the attributes, and the value of 1 was assigned in the

value column through the field calculator. The value of "water field" became 1, and then the other values were set to 0. Finally, through the surface to raster tool, the threat raster of "water field" was output. Other threat raster operations were performed as above.

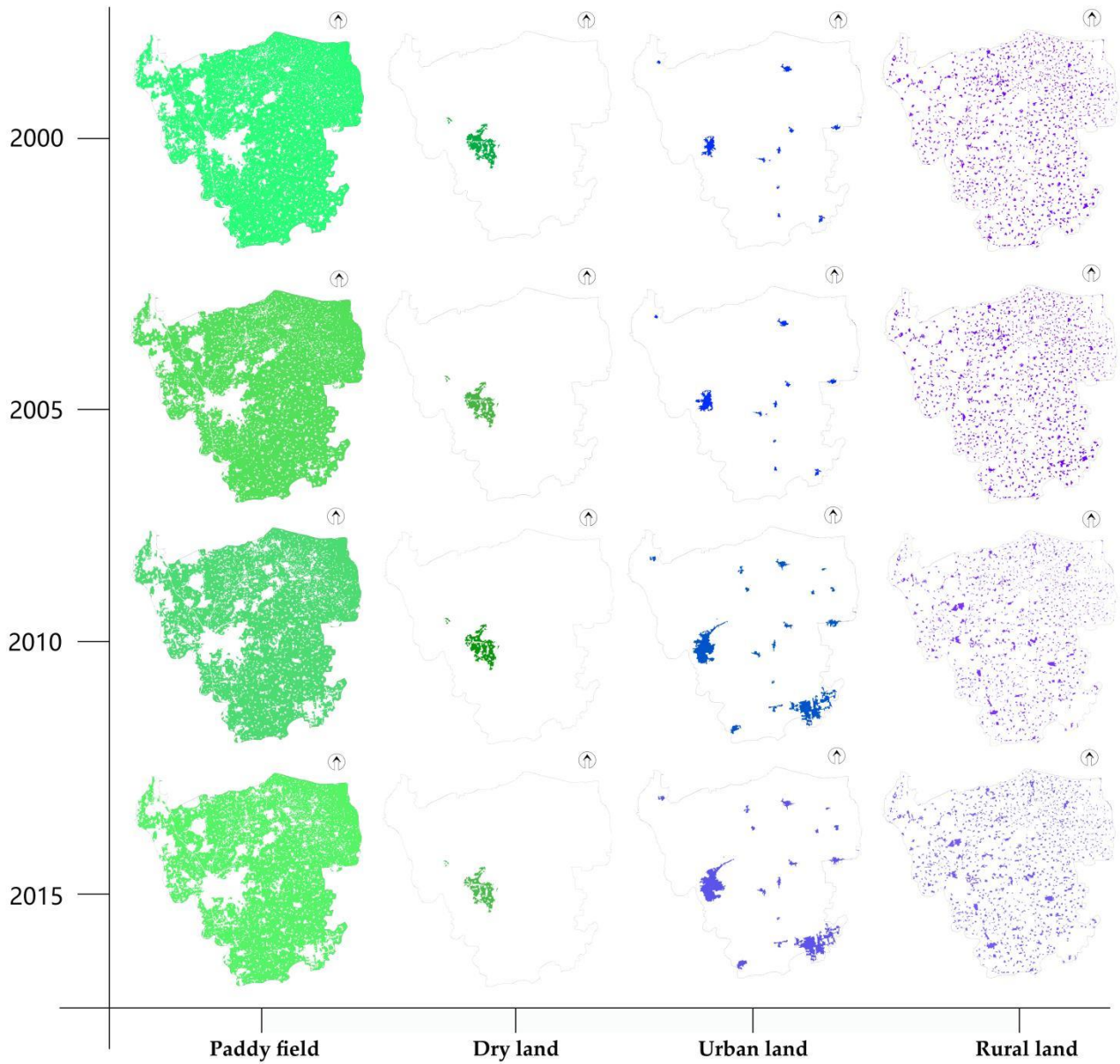


Figure S.1 Threat rasters

Table S.2 Parameters of the threat factors affecting the habitat quality.

Threat Factor	Maximum distance	Weight	Spatial decay type
---------------	------------------	--------	--------------------

Paddy Field	3	0.7	Linear
Dryland	3	0.7	Linear
Urban land	5	0.2	Exponential
Rural land	4.5	0.3	Exponential

where Maximum distance is the maximum distance over which each threat affects habitat quality, Weight is the impact of each threat on habitat quality, Spatial decay type is the type of decay over space for each threat. The parameters are taken from the InVEST modelling manual and previous research (Bai et al., 2020; Zhu et al., 2020; Liu et al., 2021).

Table S.3 Sensitivity of LULC types to each threat factor.

LULC	Name	Habitat suitability	Threat factor			
			Water Field	Dryland	Urban land	Rural land
11	Paddy Field	0.5	0.25	0.3	0.5	0.4
12	Dryland	0.4	0.3	0.25	0.5	0.4
24	Woodland	1	0.7	0.8	1	0.85
31	Grassland	0.7	0.6	0.7	0.8	0.7
41	Canal	0.8	0.7	0.65	0.75	0.7
42	Lake	0.8	0.65	0.65	0.75	0.7
43	Reservoir pit	0.8	0.65	0.6	0.75	0.7
46	Beach land	0.7	0.5	0.5	0.75	0.7
51	Urban land	0	0	0	0	0

where Habitat suitability is the suitability of this LULC class as habitat, Threat factors are the relative sensitivity of each LULC class to each type of threat. The parameters are taken from the InVEST modelling manual and previous research (Liu et al., 2021; Nie et al., 2021; Wang and Cheng, 2022).

(3) Soil retention (SR)

The Sediment Delivery Ratio module required inputs such as DEM, rainfall erosivity index (R), soil erodibility (K), LULC, P and C coefficients, watersheds, threshold flow accumulation, Borselli K parameter, Borselli IC0 parameter, maximum SDR value, maximum L value.

The rainfall erosivity factor (R) reflects the effects of rainfall frequency, rainfall intensity, rainfall duration, and runoff volume on soil erosion. This study used equations based on the average monthly rainfall datasets (J. R. Williams et al., 1984).

$$R = \sum_1^{12} 1.735 \times 10^{[1.5 \times \log_{10} \left(\frac{P_i^2}{P} \right) - 0.08188]}$$

where R is the rainfall erosivity factor [MJ·mm/(km²·h·a)], P_i is the monthly rainfall (mm), and P is the annual rainfall (mm).

The soil erodibility factor (K) indicates the susceptibility to soil detachment or soil particle transport caused by rainfall (Figure S.2). The formula was as follows:

$$K = 0.1317 \times \left\{ \left(0.2 + 0.3 \times \exp \left[-0.0256 \times SAN \times \left(1 - \frac{SIL}{100} \right) \right] \right) \times \left(\frac{SIL}{CLA + SIL} \right)^{0.3} \right. \\ \times \left(1.0 - \frac{0.25 \times OM}{OrgC + \exp(3.72 - 2.95 \times OM)} \right) \\ \left. \times \left(1.0 - \frac{0.75 \times SN}{SN + \exp(-5.51 + 22.9 \times SN)} \right) \right\}$$

where K is the soil erodibility factor, SN=1.0-SAN/100, OM, SIL, SAN, and CLA are the percentage contents of organic matter, silt, sand, and clay, respectively.

The LS factor reflects the combined effect of slope length and slope gradient on soil erosion and is dimensionless (J. R. Williams et al., 1984). The formula was as follows:

$$L = (\lambda/22.13)^m$$

$$m = \beta / (1 + \beta)$$

$$\beta = (\sin \theta / 0.089) / [3.0 \times (\sin \theta)^{0.8} + 0.56]$$

$$S = \begin{cases} 10.8 \times \sin \theta + 0.03 & \theta < 5.14^\circ \\ 16.8 \times \sin \theta - 0.5 & 5.14^\circ \leq \theta < 10.20^\circ \\ 21.91 \times \sin \theta - 0.96 & 10.20^\circ \leq \theta \end{cases}$$

where L is the slope length factor, S is the slope factor, m is the slope length index, θ is the slope angle ($^\circ$), and λ is the slope length (m).

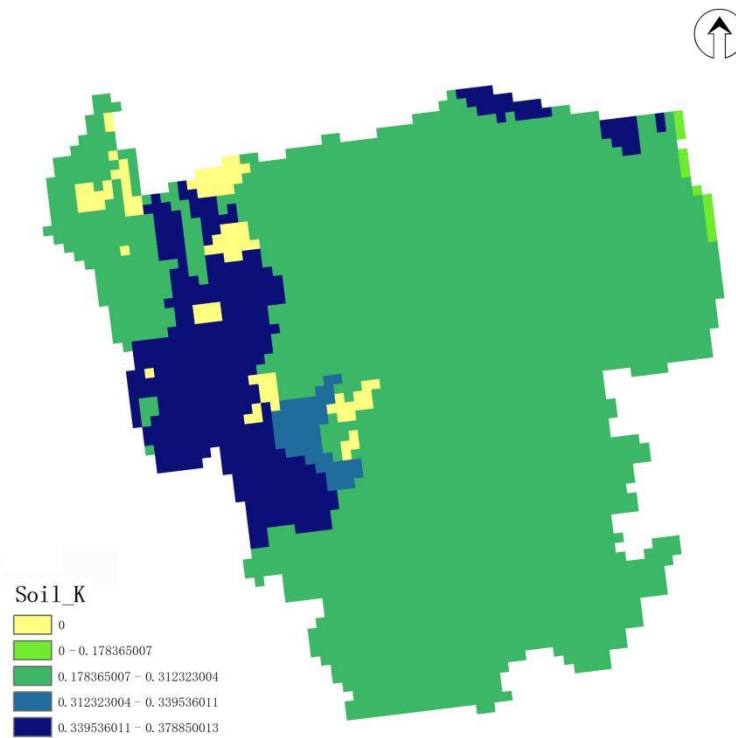


Figure S.2 Soil Erodibility (K)

Factor C demonstrates land cultivation practices and measures to prevent soil erosion (Mati et al., 2000). Factor P indicates conservation measures used to control runoff, reduce runoff rates, change runoff patterns, etc. The relevant parameters were obtained by using the manual and related literature (Feng et al., 2022; Ma et al., 2022; Yang et al., 2023), as shown in Table S.4.

Table S.4 Land cover classification of the C and P factors.

LULC_name	lucode	C	P
Paddy field	11	0.23	1
Dry land	12	0.31	0.4

Woodland	24	0.05	0.2
Grassland	31	0.14	0.2
Canal	41	0	0
Lake	42	0	0
Reservoir pit	43	0	0
beach land	46	0	0
Urban land	51	0	0
Rural land	52	1	0.15
Other construction land	53	0	0

(4) Water yield (WY)

The data to be entered into the water production module included: precipitation, evapotranspiration, root restricting layer depth, plant available water content, LULC, watersheds, biophysical table, and Z parameter.

The annual potential evapotranspiration was calculated using the Modified-Hargreaves method (Wang et al., 2019) with the following formula:

$$ET_0 = 0.0013 \times 0.408 \times RA \times (T_{avg} + 17) \times (TD - 0.0123P)^{0.76}$$

Where RA is the radiation from the top of the solar atmosphere, T_{avg} is the average daily maximum and minimum temperatures, TD is the Interpolation of average daily maximum and minimum temperatures, and P is the average monthly precipitation.

The depth of the root restricting layer was rendered and exported based on database field lookups. The plant available water content indicated the effective soil water content (Figure S.3), which could be calculated from the soil texture and soil organic matter content. The calculation formula was as follows:

$$PAWC = 54.509 - 0.132sand\% - 0.003(sand\%)^2 - 0.055silt\% - 0.006(silt\%)^2 - 0.738clay\% + 0.007(clay\%)^2 - 2.688OM\% + 0.501(OM\%)^2$$

where sand% is the proportion of soil grit, silt% is the proportion of soil powder particles, clay% is the proportion of soil clay particles, and OM is the Soil organic matter content.

The biophysical table was obtained through literature studies (Feng et al., 2012; Liu et al., 2020; Guo et al., 2021; Zhang et al., 2021) and references to modelling manuals (Table S.5), and the Z coefficients were seasonal constants with a range of values from 1 to 30.

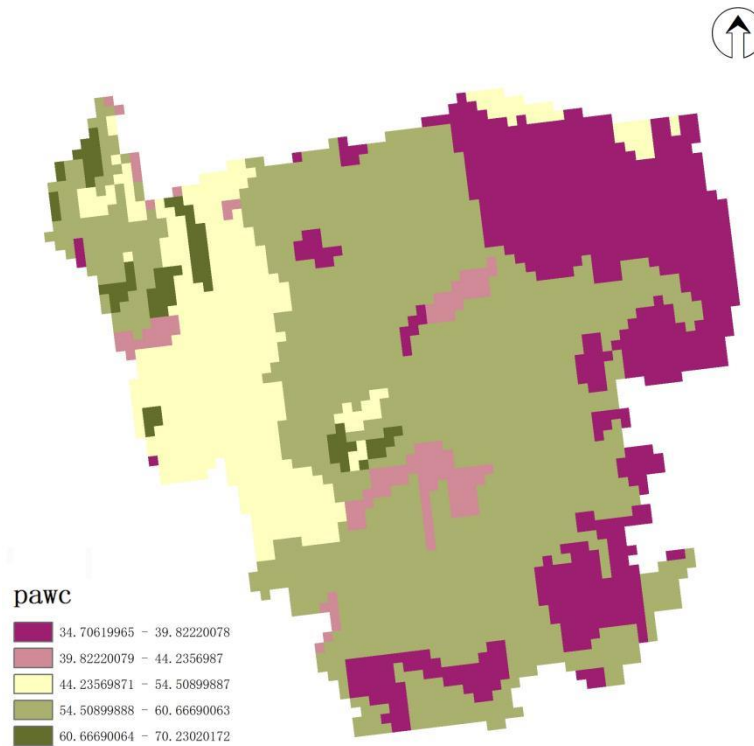


Figure S.3 Plant available water content

Table S.5 Biophysical Table in water yield module of Xinghua.

lucode	LULC_desc	LULC_veg	root_depth	Kc
11	Paddy Field	1	2100	1.1
12	Dry land	1	2100	0.65
24	Woodland	1	7000	1
31	Grassland	1	2600	0.65
41	Canal	0	1000	1

42	Lake	0	1000	1
43	Reservoir pIT	0	1000	1
46	Beach land	0	1000	1
51	Urban land	0	300	0.3
52	Rural land	0	400	0.4
53	Other construction land	0	300	0.3

The annual water yield for each raster cell is precipitation minus actual evapotranspiration. The formula was as follows:

$$Y_x = \left(1 - \frac{AET_x}{P_x}\right) \cdot P_x$$

where Y_x is the annual water yield of grid cell x (mm), AET_x is the actual annual evaporation (mm) from grid x , and P_x is the average annual precipitation (mm) for raster x .

(5) Crop product supply (CP)

The data to be entered into the water production module included: LULC, LULC to crop table, and fertilization rate table.

References

- Bai, Y., Chen, Y., Alatalo, J. M., Yang, Z., and Jiang, B. (2020). Scale effects on the relationships between land characteristics and ecosystem services- a case study in Taihu Lake Basin, China. *Science of The Total Environment* 716, 137083. doi: 10.1016/j.scitotenv.2020.137083.
- Cai, W., and Peng, W. (2021). Exploring Spatiotemporal Variation of Carbon Storage Driven by Land Use Policy in the Yangtze River Delta Region. *Land* 10, 1120. doi: 10.3390/land10111120.
- Feng, J., Chen, F., Tang, F., Wang, F., Liang, K., He, L., et al. (2022). The Trade-Offs and Synergies of Ecosystem Services in Jiulianshan National Nature Reserve in Jiangxi Province, China. *Forests* 13, 416. doi: 10.3390/f13030416.
- Feng, X. M., Sun, G., Fu, B. J., Su, C. H., Liu, Y., and Lamparski, H. (2012). Regional effects of vegetation restoration on water yield across the Loess Plateau, China. *Hydrol. Earth Syst. Sci.* 16, 2617–2628. doi: 10.5194/hess-16-2617-2012.

- Guo, M., Ma, S., Wang, L.-J., and Lin, C. (2021). Impacts of future climate change and different management scenarios on water-related ecosystem services: A case study in the Jianghuai ecological economic Zone, China. *Ecological Indicators* 127, 107732. doi: 10.1016/j.ecolind.2021.107732.
- Hu, X., Hou, Y., Li, D., Hua, T., Marchi, M., Paola Forero Urrego, J., et al. (2023). Changes in multiple ecosystem services and their influencing factors in Nordic countries. *Ecological Indicators* 146, 109847. doi: 10.1016/j.ecolind.2022.109847.
- J. R. Williams, C. A. Jones, and P. T. Dyke (1984). A Modeling Approach to Determining the Relationship Between Erosion and Soil Productivity. *Transactions of the ASAE* 27, 0129–0144. doi: 10.13031/2013.32748.
- Liu, H., Zheng, L., Wu, J., and Liao, Y. (2020). Past and future ecosystem service trade-offs in Poyang Lake Basin under different land use policy scenarios. *Arab J Geosci* 13, 46. doi: 10.1007/s12517-019-5004-x.
- Liu, S., Ren, H., Shi, X., Pan, J., and Wang, H. (2010). Different Methods for Prediction of Spatial Patterns of Paddy Soil Organic Carbon Density in Changxing County, Zhejiang Province: Different Methods for Prediction of Spatial Patterns of Paddy Soil Organic Carbon Density in Changxing County, Zhejiang Province. *Geo-information Science* 12, 180–185. doi: 10.3724/SP.J.1047.2010.00180.
- Liu, Y., Xu, B., Hu, Q., and Li, J. (2021). Evaluation of Habitat Quality in Lanzhou Region Based on InVEST Model. in *2021 28th International Conference on Geoinformatics* (Nanchang, China: IEEE), 1–6. doi: 10.1109/IEEECONF54055.2021.9687658.
- Ma, B., Zeng, W., Xie, Y., Wang, Z., Hu, G., Li, Q., et al. (2022). Boundary delineation and grading functional zoning of Sanjiangyuan National Park based on biodiversity importance evaluations. *Science of The Total Environment* 825, 154068. doi: 10.1016/j.scitotenv.2022.154068.
- Mati, B. M., Morgan, R. P., Gichuki, F. N., Quinton, J. N., Brewer, T. R., and Liniger, H. P. (2000). Assessment of erosion hazard with the USLE and GIS: A case study of the Upper Ewaso Ng'iro North basin of Kenya. *International Journal of Applied Earth Observation and Geoinformation* 2, 78–86. doi: 10.1016/S0303-2434(00)85002-3.
- Nie, M., Huang, S., Pu, L., Zhu, M., and Qie, L. (2021). Spatial and Temporal Dynamics and Trade-offs and Synergies Analysis of Ecosystem Services in Rapidly Urbanizing Areas: A Case Study of the Su-Xi-Chang region Resour. *Resour. Environ. Yangtze Val.* 30, 1088–1099. doi: 10.11870/cjlyzyhj202105006.
- Wang, B., and Cheng, W. (2022). Effects of Land Use/Cover on Regional Habitat Quality under Different Geomorphic Types Based on InVEST Model. *Remote Sensing* 14, 1279. doi: 10.3390/rs14051279.
- Wang, Y., Wang, D., Qian, J., and Gao, S. (2021). Study on planning and benefit analysis of returning polder area to lakes in plain water network area—a case study of Lixiahe Lake areas in Xinghua County. *Jiangsu Water Resources*. 16-18+24. doi: 10.16310/j.cnki.jssl.2019.05.005.

Yang, Q., Zhang, P., Qiu, X., Xu, G., and Chi, J. (2023). Spatial-Temporal Variations and Trade-Offs of Ecosystem Services in Anhui Province, China. *IJERPH* 20, 855. doi: 10.3390/ijerph20010855.

Zhang, X., Zhang, G., Long, X., Zhang, Q., Liu, D., Wu, H., et al. (2021). Identifying the drivers of water yield ecosystem service: A case study in the Yangtze River Basin, China. *Ecological Indicators* 132, 108304. doi: 10.1016/j.ecolind.2021.108304.

Zhou, R., Lin, M., Gong, J., and Wu, Z. (2019). Spatiotemporal heterogeneity and influencing mechanism of ecosystem services in the Pearl River Delta from the perspective of LUCC. *J. Geogr. Sci.* 29, 831–845. doi: 10.1007/s11442-019-1631-0.

Zhu, C., Zhang, X., Zhou, M., He, S., Gan, M., Yang, L., et al. (2020). Impacts of urbanization and landscape pattern on habitat quality using OLS and GWR models in Hangzhou, China. *Ecological Indicators* 117, 106654. doi: 10.1016/j.ecolind.2020.106654.